

# Wideband Hexagonal Fractal Antenna on Epoxy Reinforced Woven Glass Material

M. A. Dorostkar<sup>1</sup>, R. Azim<sup>2</sup>, M. T. Islam<sup>1</sup>, and Z. H. Firouzeh<sup>3</sup>

<sup>1</sup>Department of Electrical, Electronic & Systems Engineering  
Universiti Kebangsaan Malaysia, 43600 UKM Bangi, Malaysia

<sup>2</sup>Department of Physics  
University of Chittagong, Chittagong 4331, Bangladesh  
rezaulazim@yahoo.com

<sup>3</sup>Department of Electrical & Computer Engineering  
Isfahan University of Technology, Isfahan, Iran

**Abstract**— In this paper a novel hexagonal-circular Fractal antenna is proposed for wideband applications. The proposed antenna is made of iterations of a circular slot inside a hexagonal metallic patch with a transmission line and is fabricated on low cost epoxy matrix reinforced woven glass material. Measurement shows that with a dimension of  $0.36\lambda_0 \times 0.36\lambda_0 \times 0.0071\lambda_0$  (where  $\lambda_0$  is the lower edge frequency of the operating band), the proposed antenna achieves a wide impedance bandwidth ranging from 1.34 GHz to 3.44 GHz (88%). The proposed antenna also achieves high gain and exhibits a stable radiation pattern which makes it suitable for many wireless communications such as DCS-1800, PCS-1900, IMT-2000/UMTS, ISM (including WLAN), Wi-Fi and Bluetooth.

**Index Terms** — DCS, Epoxy material, Fractal geometry, ISM, wideband, Wi-Fi.

## I. INTRODUCTION

Recent developments in wireless communication have heightened the need for wideband antennas with compact size and low cost. An antenna is considered as a wideband antenna if its impedance and pattern do not change significantly over about an octave or more. Several methods and approaches have been reported for designing antennas with wide and ultra-wide operating band in which the periodic structure is one of the most common methods [1-3]. Periodic

geometry has been studied using the fundamental concept of Fractal structure for the last few decades. Self-similarity and space filling are two common properties for designing of Fractal antennas. Self-similarity leads to multiband while the space filling causes the long electrical length. If the antenna dimensions are smaller than a quarter of wavelength, it cannot be an efficient design because of decreasing of radiation resistances [1-5].

Most studies in the field of Fractal antenna have focused on Koch, Sierpinski and Hilbert, Cantor, Minkowski and Fractal tree shapes in recent years. The Koch monopole antenna is designed by iterating the initial triangle pulse [6]. The Log periodic Fractal Koch antenna for UHF band application is proposed in [7]. Koch like sided Sierpinski Gasket multi-Fractal dipole antenna is one of the most important Fractal antennas based on the triangle shape and is suitable for multi-band application [8]. In designing of the antenna proposed in [9], the Sierpinski Fractal shape is perturbed and two iteration stages had been introduced to achieve dual band centered at 915 MHz and 1.575 GHz. To yield multiband behavior, the antenna proposed in [10] considered two Fractal stages of the Sierpinski Gasket as base shape. With an overall size of  $60 \times 80$  mm, the proposed antenna achieved dual operating bands centered at 898 MHz and 2.44 GHz. By taking the planar Sierpinski prefractal as a reference shape, the antenna proposed in [11] achieved a multiband behavior

with a dimension of  $80 \times 80$  mm. In [12], a modified Fractal slot antenna was presented for DCS, WiMAX and IMT applications. By applying Minkowski Fractal concept, the reported antenna achieved dual operating band of 1.71-1.88 GHz and 3.2-5.5 GHz. Despite having fairly compact dimensions ( $38.54 \times 75.2$  mm), this antenna requires a complex structure to create and control dual operating band. The CPW-fed slot antenna proposed in [13] is based on hexagonal Fractal geometry and only applicable for the UWB frequency band. However, the realized gain of this antenna is quite low. In [14], the hexagonal shape is obtained by three iterations with arranging dipole configuration that is large in physical size. By using side-fed feeding configuration to the hexagonal geometry, the antenna proposed in [15] achieved an impedance bandwidth of 2.5 GHz (1.1-3.6 GHz). However, the reported antenna does not possess a physical compact profile having a dimension of  $150 \times 150$  mm. To achieve an operating band ranging from 1.9-2.4 GHz, two parallel slots were incorporated into the patch of a microstrip antenna proposed in [16]. However, the designed antenna is not suitable for portable mobile devices due to its large volumetric size of  $140 \times 210 \times 10$  mm. Tapering the radiating patch or ground plane shape and use of lossy substrates have also been reported in achieving wide and ultra-wide band frequency response [17-18]. Despite of wide and ultra-wide operating band, none of these reported Fractal antennas deal with hexagonal circular geometry which could be a new arena in the designing of Fractal antenna.

In this paper, a novel wideband Fractal antenna based on hexagonal-circular geometry is proposed and designed on epoxy matrix reinforced woven glass material. The iterations of a circular slot inside a hexagonal metallic patch fed by a transmission line help to achieve wide impedance bandwidth ranging from 1.34 to 3.44 GHz. The achieved high gain and stable radiation patterns makes the proposed suitable for being used in various wireless applications such as DCS-1800 (1710-1880 MHz), PCS-1900 (1850-1990 MHz), IMT-2000/UMTS (1885-2200 MHz), ISM (2400-2483 MHz), Wi-Fi (2400 MHz) and Bluetooth

(2400-2500 MHz). Compared to the antennas reported in [11-12, 15-16], the proposed antenna is compact, simple and easy to fabricate.

## II. ANTENNA DESIGN

The proposed antenna designed on substrate material consists of an epoxy matrix reinforced woven glass. The fiber glass in the composition is 60% while the epoxy resin contributes 40% of the composition. This composition of epoxy resin and fiber glass varies in thickness and is direction dependent. One of the attractive properties of polymer resin composite is that they can be shaped and reshaped repeatedly without losing their material properties [19]. Due to ease of fabrication, design flexibility, low manufacturing cost and market availability, the epoxy matrix reinforced woven glass material has become popular in the designing of microstrip patch antenna.

The design of the proposed antenna is based on a hexagonal geometry. In the proposed shape, the initial shape is a subtraction of hexagonal shape with a length of  $(R_1 + d_1)/(\sqrt{3}/2)$  and circle with radius  $R_1$ , where  $d_1$  is the thickness between hexagonal and circle, and is as shown in Fig. 1 (a). The existence of edges leads to losses of energies, so the internal geometry has been changed to circular. The next shape is the subtraction of hexagonal with a length of  $(R_2 + d_2)/(\sqrt{3}/2)$  and circle with radius  $R_2$ , while it rotates by  $30^\circ$ . This process is continued to seven steps, and in every step the shapes are rotated  $30^\circ$ . The shape can rotate clockwise or counterclockwise due to the symmetrical nature of the proposed shape. If the proposed shape is chosen to rotate in a clockwise (counterclockwise), the other shapes should be rotated clockwise (counterclockwise). For limiting 3D modulator error, the next iterations are constructed so that it introduces interference between the main patch and next iteration. The metallic concentration between the iterations (hexagonal and circle) is about 0.1mm. The configuration is the iterations of a circular slot inside a hexagonal metallic patch. Figure 1 shows the shapes and relations based on their distances from the center and design procedure of proposed Fractal structured geometry.

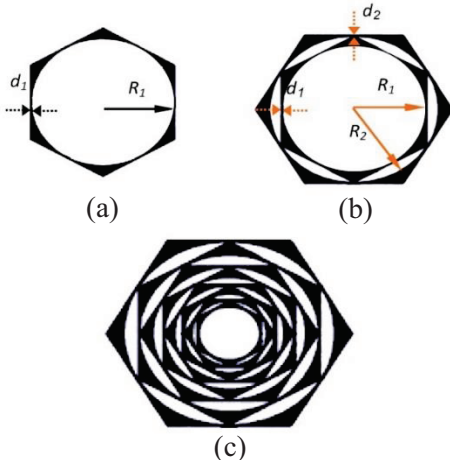


Fig. 1. Design procedure of the proposed Fractal geometry: (a) base shape, (b) first iteration, and (c) final shape.

The variation of return loss for various iterations is shown in Fig. 2. It is seen that the antenna with higher iteration exhibits better impedance bandwidth. It is also observed that the base shape with iteration (Itr) 0 has a narrow bandwidth which permits to continue the iterations up to seven to obtain a wider operating bandwidth.

Five parameters are considered for the design of hexagonal geometry including  $R_i$  (length of hexagonal and circular),  $d_i$  (difference between the lengths of hexagonal and circle),  $L_T$  (length of transmission line),  $L_G$  (side length of ground plane), and  $W_T$  (width of the transmission line) that their relations are based on the following equations:

$$R_{i+1} = \frac{R_i + d_i}{\sqrt{3}} \quad i = 1, 2, 3, \dots, N, \quad (1)$$

and the vertical gap between the ground plane and the radiating element is:

$$h = L_T - L_G. \quad (2)$$

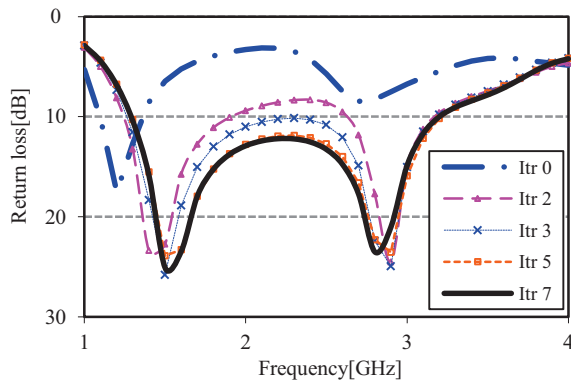


Fig. 2. Return loss curves for various iterations.

The configuration of the proposed antenna is shown in Fig. 3. The hexagonal Fractal patch is printed on one side of a 1.6-mm thick epoxy woven glass material of relative permittivity 4.6, while the partial ground plane with side length  $L_G$  is printed on the other side. The hexagonal patch with side length  $R_{16}$  is fed by a transmission line. The length and width of the transmission line are fixed at  $L_T$  and  $W_T$  respectively to achieve  $50\Omega$  characteristic impedance. An SMA is connected to the transmission line. The overall electrical dimension of the proposed antenna is  $0.36\lambda_0 \times 0.36\lambda_0 \times 0.0071\lambda_0$  (where  $\lambda_0$  is the lower edge of the operating band), which is smaller than the antenna proposed in [11, 16] for DCS, PCS, IMT/UMTS, and ISM applications.

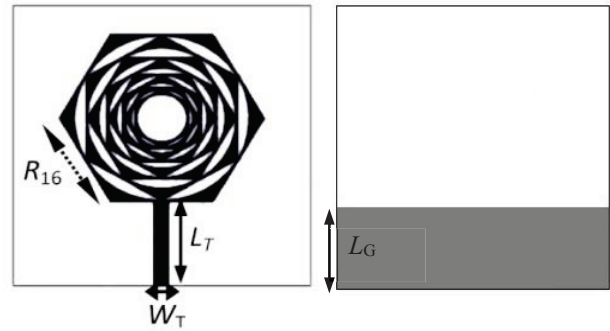


Fig. 3. Configuration of the proposed antenna: (a) top view (left side), and (b) bottom view (right side).

### III. ANTENNA SPECIFICATIONS

The dimension of the perimeter of a hexagonal is equal 1 ( $D = 1$ ) and hexagonal area is called  $S_{\text{hexagonal}}$  with dimension of 2 ( $D = 2$ ), so the dimensions of the proposed shape are between 1 and 2 ( $1 < D < 2$ ). Due to existing of two types of shapes (hexagonal and circular), the dimension of the proposed geometry is not able to be figured out only by one scale factor. In the first step, the equivalent hexagonal shape with circular shape can be calculated according to the relation (4). Then the dimension of the new proposed Fractal shape can be computed according to the relation (6).  $(1.5\sqrt{3}) \times (R_1^2 - R_n^2)$  is scale factor where  $R_1$  is the length of the first hexagonal and  $R_n$  is the length of the equivalent hexagonal with the circle radius of  $n$ th iterations.

$S_n$  is the area of the  $n$ th iterations that is determined with relation (5). The hexagonal area  $S_{\text{hexagonal}}$  is defined as:

$$S_{hexagonal} = \frac{3\sqrt{3}}{2} R_1^2. \quad (3)$$

$R_n$ , the length of the corresponding hexagonal with a circle radius of  $n$ th iterations can be written as:

$$R_n = \sqrt{\frac{2\pi}{3\sqrt{3}}} \left[ R_{n-1} \cos\left(\frac{\pi}{6}\right) - d \right], n=2, 3, 4,.. \quad (4)$$

The area corresponding to the hexagon-circular Fractal area of  $n$ th iterations is:

$$S_{hexagonal} - S_n = \frac{3\sqrt{3}}{2} (R_1^2 - R_n^2), \quad (5)$$

$$D = \frac{\text{Log}(S_{hexagonal} - S_n)}{\text{Log}\{1.5\sqrt{3} \times (R_1^2 - R_n^2)\}}. \quad (6)$$

The first design is done with  $R_{16} = 27.6$  mm and  $d = 0.5$  mm, that  $d$  is constant for all the iterations. The dimensions for the proposed geometry to 7 iterations are arranged in Table 1. It can be observed that increasing iterations enhance the dimension, so lead to increasing the electrical length.

Table 1: Dimension of the proposed Fractal geometry for various iterations

|                |            |        |        |         |
|----------------|------------|--------|--------|---------|
| Iteration      | Base Shape | First  | Second | Third   |
| Dimension (mm) | 1.0025     | 1.1389 | 1.2303 | 1.3040  |
| Iteration      | Fourth     | Fifth  | Sixth  | Seventh |
| Dimension (mm) | 1.3692     | 1.4302 | 1.4895 | 1.5488  |

#### IV. PARAMETRIC STUDY

A parametric study is conducted to investigate the effects of the different parameters on the antenna performances. All the parametric studies have been conducted using high frequency simulation software from Ansoft. In the simulation, only the parameter of interest has been changed and the other parameters are kept constant using of the objective function  $S_\lambda(f)$  with the strategy of  $S_\lambda(f) < -10$ , where  $S_\lambda(f)$  is function of return loss with specified parameters,  $\lambda = \{L_T, L_G, W_T, R_{16}, d; i=1, 2, \dots, 8\}$ , of the proposed antenna that has larger bandwidth.

The variation of the return loss with  $\lambda$  parameter is shown in Fig. 4. It is observed that decreasing and increasing of  $\lambda$  from a certain value leads to decrease in the bandwidth. Table 2 summarizes the effects of  $\lambda$  on bandwidth performances with various values.

The variations of the return loss with  $R_{16}$  (length of last hexagonal structure) are shown in Fig. 5. It is observed that decreasing and increasing of  $R_{16}$  from

a certain value leads to decrease in the bandwidth. It can be seen from the Fig. 5, that a value of 27.6 mm for  $R_{16}$  can maintain the good impedance bandwidth with better return loss values. The variation of the return loss with  $L_T$  (length of transmission line) is depicted in Fig. 6.

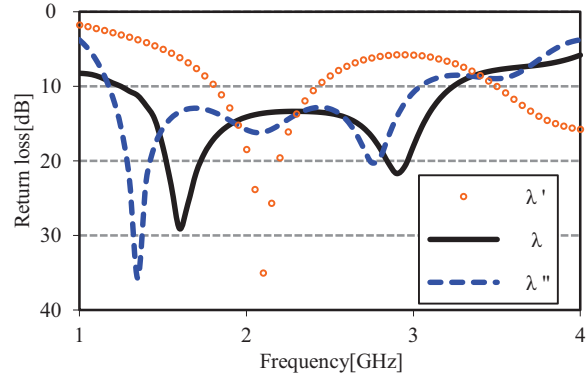


Fig. 4. Effect of  $\lambda$  on return loss characteristics.

Table 2: Variation values for all  $\lambda$  parameters

| Parameter(mm) | $\lambda'2$ | $\lambda2$ | $\lambda''2$ |
|---------------|-------------|------------|--------------|
| $L_T$         | 27          | 24         | 20           |
| $L_G$         | 26          | 23         | 19           |
| $W_T$         | 4           | 3.3        | 2            |
| $R_{16}$      | 30          | 27.6       | 20           |
| $d_1$         | 0.4         | 0.47       | 0.36         |
| $d_2$         | 0.67        | 0.3        | 0.445        |
| $d_3$         | 0.45        | 0.65       | 0.4          |
| $d_4$         | 0.45        | 0.35       | 0.68         |
| $d_5$         | 0.42        | 0.4        | 0.49         |
| $d_6$         | 0.35        | 0.4        | 0.32         |
| $d_7$         | 0.5         | 0.44       | 0.5          |
| $d_8$         | 0.42        | 0.5        | 0.42         |

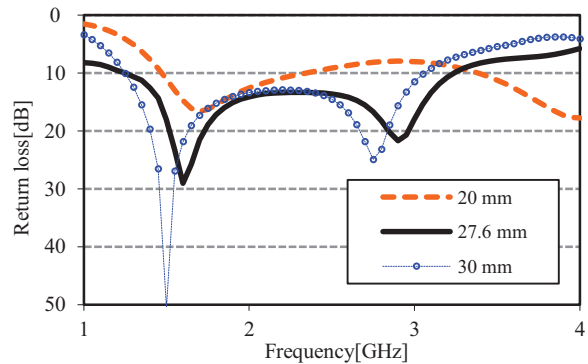


Fig. 5. Effect of  $R_{16}$  on return loss characteristics.

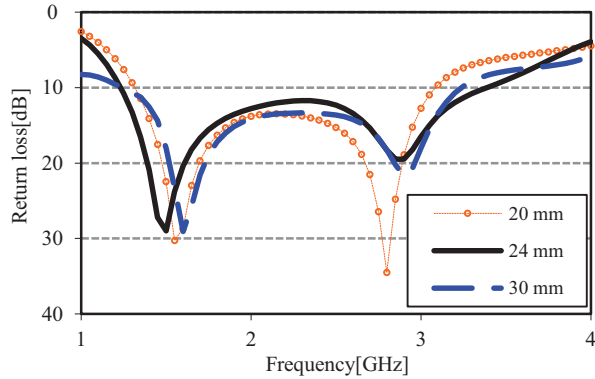


Fig. 6. Effect of  $L_T$  on return loss characteristics.

In the simulation of performance analysis of  $L_T$  versus frequency, only the value of  $L_T$  is varied while the other parameters are kept constant at  $R_{l6} = 27.6$  mm,  $W_T = 3.3$  mm,  $L_G = 23$  mm and  $h = 1$  mm. It is seen from the plot that decreasing of  $L_T$  leads to decrease in the operating bandwidth, while increasing of  $L_T$  leads to increase in operating bandwidth. It is also noted that, decreasing and increasing of  $L_T$  from a certain value leads to a mismatch of the input impedance. Based on the observations, it is found that a value of 24 mm is an appropriate choice for  $L_T$  in achieving the widest operating bandwidth.

Figure 7 shows the variations of the return loss characteristics with the width of the transmission line,  $W_T$ . In optimization, only the value of  $W_T$  is varied while the other parameters are kept constant at  $R_{l6} = 27.6$  mm,  $L_T = 24$  mm,  $L_G = 23$  mm and  $h = 1$  mm. It is seen from the figure that, decreasing and increasing of the  $W_T$  leads to decrease the impedance bandwidth. It is also observed that, when  $W_T$  decreases and increases from a certain value, the impedance matching becomes poor at higher frequencies resulting in a bandwidth reduction. In this design, a width of 3.3 mm performs with better return loss and input impedances.

The variation of return loss with  $h$  parameter (the vertical gap between the ground plane and the radiating element) is shown in Fig. 8. It can be observed that, increasing and decreasing of  $h$  from the certain value leads to decrease in the bandwidth. From the plot in Fig. 8, it is clear that a gap of 1 mm can maintain the good impedance bandwidth with better return loss values.

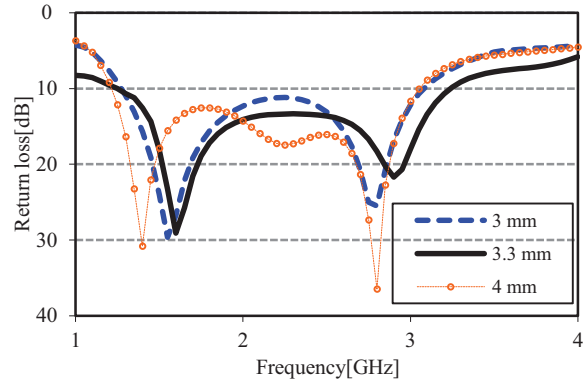


Fig. 7. Effect of  $W_T$  on return loss characteristics.

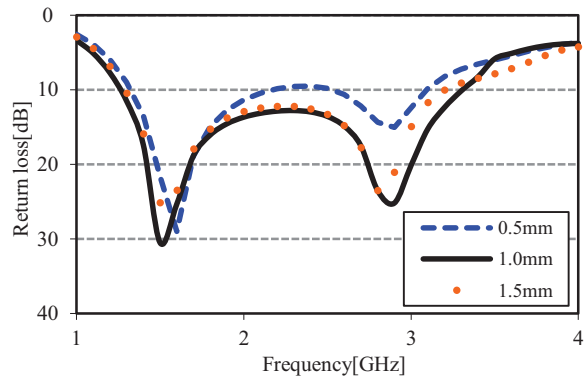


Fig. 8. Effect of  $h$  on return loss characteristics.

## V. RESULTS AND DISCUSSION

The characteristics of the proposed antenna have been optimized by high frequency simulation software HFSS. A prototype with optimized dimensions tabulated in Table 3 has subsequently been fabricated for experimental verification and shown in Fig. 9. The antenna performances have been measured in an anechoic chamber using far field antenna measurement system and Agilent E8362C Vector Network Analyzer. The experimental setup was calibrated carefully by considering the effect of feeding cable using an Agilent digital calibration kit.

The simulated and measured return losses and VSWR of the proposed antenna are depicted in Fig. 10. It is observed from the plot that the measured impedance bandwidth of the proposed antenna is ranging from 1.34 to 3.44 GHz, which is equivalent 88%. A good agreement between the simulated and

measured results has been observed. The disparity between the measured and simulated results especially at edge frequencies is attributed to manufacturing tolerance and imperfect soldering effect of the SMA connector.

Table 3: Optimized antenna parameters

| Parameter | Value (mm) | Parameter | Value (mm) |
|-----------|------------|-----------|------------|
| $L_T$     | 30         | $d_3$     | 0.65       |
| $L_G$     | 23         | $d_4$     | 0.35       |
| $W_T$     | 3.3        | $d_5$     | 0.4        |
| $R_{16}$  | 27.6       | $d_6$     | 0.4        |
| $d_1$     | 0.47       | $d_7$     | 0.44       |
| $d_2$     | 0.3        | $d_8$     | 0.5        |



Fig. 9. Photograph of the realized Fractal antenna.

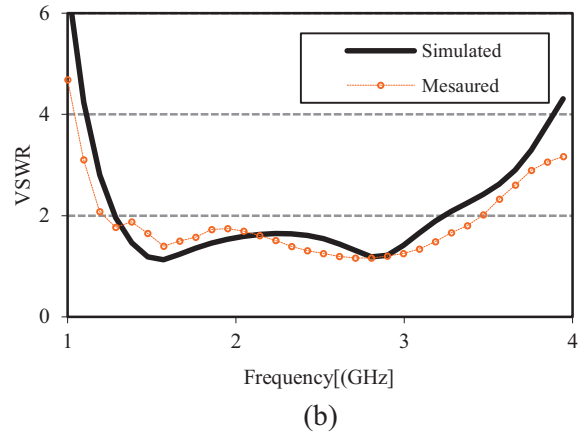
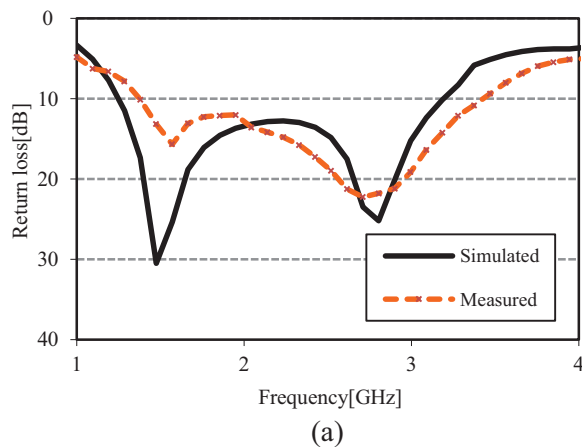


Fig. 10. Measured: (a) return loss, and (b) VSWR.

The measured phase variation of the input impedance of the proposed antenna is shown in Fig. 11. The phase variation across the entire operating band is reasonably linear, except at around 2.2 GHz. This linear variation in the phase with frequency ensures that all the frequency components of signal have the same delay, leading to same pulse distortion.

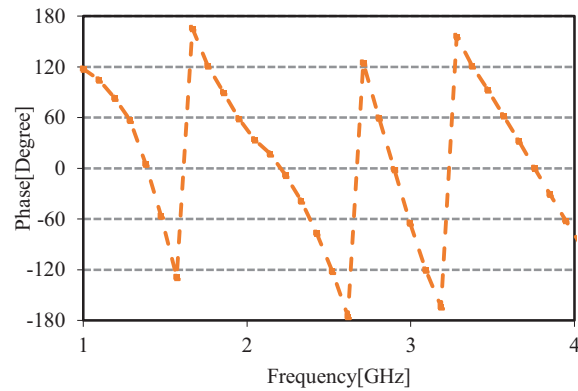


Fig. 11. Measured phase of the proposed antenna.

Figure 12 shows the peak gain and efficiency of the proposed antenna in the frequency range of 1-4 GHz. It can be observed from the figure that the antenna has a good average gain of 4.65 dBi. The maximum peak gain is 6.8 dBi at 1.34 GHz. The plot of radiation efficiency shows that the maximum radiation efficiency of the proposed antenna is 84% at 1.34 GHz and the average efficiency is 75% across the entire operating band.

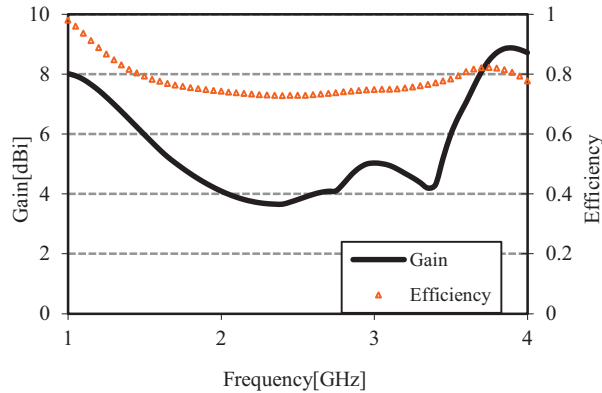


Fig. 12. Peak gain and radiation efficiency.

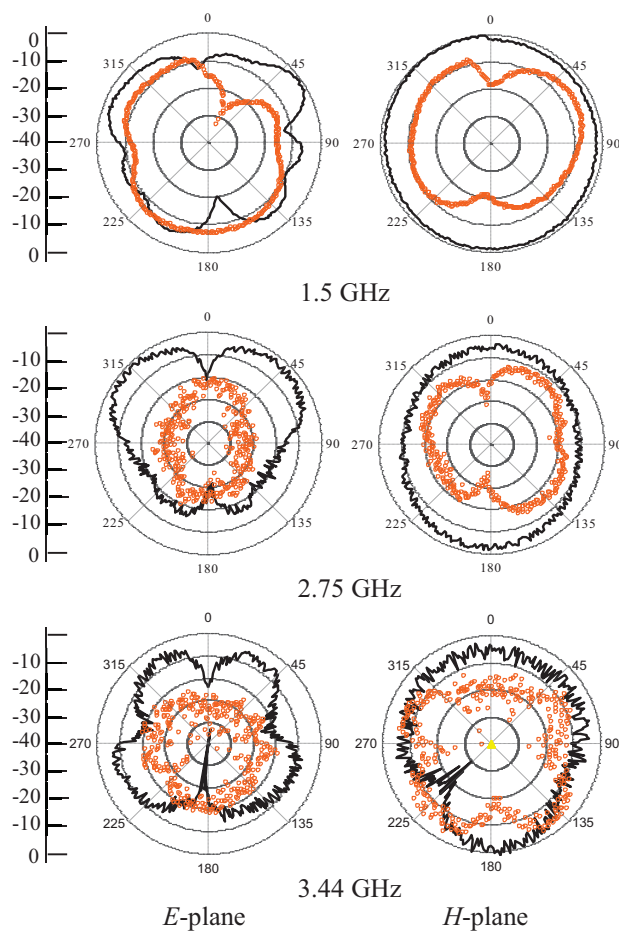


Fig. 13. Measured radiation patterns at different frequencies (black line: co-polarized field, orange line: cross-polarized field).

The measured radiation patterns of the proposed antenna at 1.5 GHz, 2.75 GHz and 3.44 GHz are depicted in Fig. 13. It can be observed from the

figure that at low frequency of 1.5 GHz both the  $E$ -plane and  $H$ -plane patterns are omnidirectional and  $H$ -plane pattern is characterized with low cross-polarization level. At higher frequencies of 2.75 GHz and 3.44 GHz, the  $E$ -plane patterns become donut shape and main beam slightly tilt away from the broad side direction due to higher order harmonic, while  $H$ -plane patterns almost retains its omni-directionality.

## VI. CONCLUSION

A novel wideband hexagonal-circular antenna has been proposed and prototyped for wideband applications. The composition of epoxy resin and fiber glass material has been used for fabrication due to their low manufacturing cost and market availability. A design evolution and a parametric study of the proposed antenna are presented to provide information for designing, optimizing and to understand the fundamental radiation mechanism. The design of the proposed antenna is simple, easy to fabricate, and very suitable to integrate into microwave circuitry due to its planar profile. Experimental results show that the proposed antenna achieved an impedance bandwidth of 2.1GHz. The nearly stable omnidirectional radiation patterns with a flat gain make the proposed antenna suitable for DCS-1800, PCS-1900, IMT-2000/UMTS, ISM, Wi-Fi and Bluetooth applications.

## ACKNOWLEDGMENT

The authors would like to thank Isfahan Mathematics House (IMH), Iran for helping this research.

## REFERENCES

- [1] C. A. Balanis, *Antenna Theory: Analysis and Design*, John Wiley & Sons, New York, 2005.
- [2] D. H. Werner and S. Ganguly, "An overview of fractal antenna engineering research," *IEEE Antennas Propagat. Mag.*, vol. 45, no. 1, pp. 38-57, 2003.
- [3] N. Cohen, "Fractal antenna application in wireless telecommunications," *Electronics Industries Forum of New England*, Boston, USA, pp. 43-49, May 1997.
- [4] J. F. Gouyet, *Physics and Fractal Structures*, Springer, Paris, France, 1996.
- [5] D. H. Werner, R. L. Haupt, and P. L. Werner, "Fractal antenna engineering: the theory and design of fractal antenna arrays," *IEEE Antennas Propagat.*

- Mag.*, vol. 41, no. 5, pp. 37-58, 1999.
- [6] N. A. Saidatul, A. A. H. Azremi, R. B. Ahmad, P. J. Soh, and F. Malek, "Multiband fractal planar inverted F antenna (F-PIFA) for mobile phone application," *Prog. Electromagn. Res. B*, vol. 14, pp. 127-148, 2009.
- [7] C. Puente, J. Romeu, R. Pous, J. Ramis, and A. Hijazo, "Small but long Koch fractal monopole," *Electron. Lett.*, vol. 34, no. 1, pp. 9-10, 1998.
- [8] M. N. A. Karim, M. K. A. Rahim, H. A. Majid, O. Ayop, M. Abu, and F. Zubir, "Log periodic fractal Koch antenna for UHF band applications," *Prog. Electromagn. Res.*, vol. 100, pp. 201-218, 2010.
- [9] F. Viani, M. Salucci, F. Robol, G. Oliveri, and A. Massa, "Design of a UHF RFID/GPS fractal antenna for logistics management," *J. Electromagn. Waves Appl.*, vol. 26, pp. 480-492, 2012.
- [10] F. Viani, M. Salucci, F. Robol, and A. Massa, "Multiband fractal ZigBee/WLAN antenna for ubiquitous wireless environments," *J. Electromagn. Waves Appl.*, vol. 26, nos. 11-12, pp. 1554-1562, 2012.
- [11] L. Lizzi, F. Viani, E. Zeni, and A. Massa, "A DVBH/GSM/UMTS planar antenna for multimode wireless devices," *IEEE Antennas Wireless Propagat. Lett.*, vol. 8, pp. 568-571, 2009.
- [12] C. Mahatthanajatuphat, P. Akhharackthalin, S. Saleekaw, and M. Krairiksh, "A bidirectional multiband antenna with modified fractal slot fed by CPW," *Prog. Electromagn. Res.*, vol. 95, pp. 59-72, 2009.
- [13] A. Azari and J. Rowhani, "Ultrawideband fractal microstrip antenna design," *Prog. Electromagn. Res. C*, vol. 2, pp. 7-12, 2008.
- [14] P. W. Tang and P. F. Wahid, "Hexagonal fractal multiband antenna," *IEEE Antennas Wireless Propagat. Lett.*, vol. 3, pp. 111-112, 2004.
- [15] K. P. Ray and S. Tiwari, "Ultra wideband printed hexagonal monopole antennas," *IET Microw. Antennas Propag.*, vol. 4, no. 4, pp. 437-445, 2010.
- [16] F. Yang, X-X. Zhang, X. Ye, and Y. Rahmat-Samii, "Wide-band E-shaped patch antennas for wireless communications," *IEEE Trans. Antennas Propagat.*, vol. 49, no. 7, pp. 1094-1100, 2001.
- [17] R. Azim, M. T. Islam, and N. Misran, "Compact tapered shape slot antenna for UWB applications," *IEEE Antennas Wireless Propagat. Lett.*, vol. 10, pp. 1190-1193, 2011.
- [18] H. W. Son, "Design of RFID tag antenna for metallic surfaces using lossy substrate," *Electron. Lett.*, vol. 44, no. 12, pp. 711-713, 2008.
- [19] I. Yarovsky and E. Evans, "Computer simulation of structure and properties of crosslinked polymers: application to epoxy resins," *Polymer*, vol. 43, no. 3, pp. 963-969, 2002.